ELSEVIER

Journal of Hazardous Materials B139 (2007) 72–78

Journal of Hazardous Materials

www.elsevier.com/locate/jhazmat

Fabrication of TiO_2/Ti electrode by laser-assisted anodic oxidation and its application on photoelectrocatalytic degradation of methylene blue

Jiaqing Li, Lei Zheng, Luoping Li, Yuezhong Xian, Litong Jin *

Department of Chemistry, East China Normal University, Shanghai 200062, China

Received 7 December 2005; received in revised form 11 May 2006; accepted 5 June 2006
Available online 10 June 2006

Abstract

A TiO_2/Ti mesh electrode by laser calcination was prepared in this article. The resulting TiO_2 film was investigated by X-ray diffraction (XRD), atomic force microscopy (AFM) and electrochemical impedance spectroscopy (EIS), and it illuminated that the prepared electrode mainly consisted of anatase TiO_2 nanoparticles on its surface and exhibited a superior photocatalytic activity. The photodegradation of methylene blue (MB) using the proposed electrode under different experimental conditions was investigated in terms of both UV absorbance at 664 nm and chemical oxygen demand (COD) removal. The electrical bias applied in photoelectrocatalytic (PEC) oxidation was also studied. The experimental results showed that under the optimal potential of +0.50 V (versus SCE), UV absorbance and COD removal during the photodegradation of MB by the proposed TiO_2/Ti mesh electrode were 97.3% and 87.0%, respectively. Through the comparison between photocatalytic (PC) oxidation and photoelectrocatalytic (PEC) oxidation, it was found that PEC oxidation was a convenient and effective way to mineralize the organic matters and that laser-treated photoelectrode exceeded the oven-treated one.

Keywords: TiO_2/Ti electrode; Photoelectrocatalysis; Laser calcination; Methylene blue (MB)

1. Introduction

Textile dyes and other industrial dyestuffs constituted one of the largest groups of organic compounds representing an increasing environmental danger [1]. Dyes were widely used and therefore wastewater was discharged into natural and domestic water systems including rivers, lakes and public sewage. As a result, they were highly contaminated [2,3]. Colored water was no longer unattractive and caused more and more complaints. Moreover, concerns were expressed about the potential toxicity of dyes and of their precursors. Environmental pollution caused by organic dyes also set a severe ecological problem, which was increased by the fact that most of them were difficult to degrade using standard methods [4]. Generally, traditional physical techniques could be employed efficiently to remove such recalcitrant pollutants. However, they were non-destructive, because they just transferred organic matter from water to sludge. This led to the requirement of regeneration of the adsorbent materials and post-treatment of solid wastes and both of them cost a lot [5].

In the last decade, advanced oxidation processes (AOPs) were used widely in the treatment of wastewater since they were able to handle the problem of organic pollutants destruction in aqueous solution [6–8]. Among AOPs, there was a great interest in the development of photocatalytic methods for degrade pollutants [9–14]. This photocatalytic method was based on the reactive properties of photogenerated electron–hole pairs. They were generated in the semiconductor (TiO_2) particles under irradiation at suitable wavelengths ($\lambda \leq 400$ nm). These electrons and holes could also recombine. Since the hole was a powerful oxidizing agent, it could decompose water and/or contaminants adsorbed on the TiO_2 surface. There were many reports on photoelectrocatalytic degradation of organic pollutants by using TiO_2 electrodes, which were prepared by coating the surfaces of electrically conducting substrates (ITO, Ti) with TiO_2 film [15–18]. In this method, positive potential was applied on the working electrode, which could inhibit the recombination of electrons and holes and enhance the rate of photoelectrocatalytic degradation of organic compounds [19–21].

Through the PC or PEC research, it was found that the photocatalytic activity of the photocatalyst TiO_2 was the key for

* Corresponding author. Tel.: +86 21 62232627; fax: +86 21 62232627.
E-mail addresses: 52040606011@student.ecnu.edu.cn (J. Li), ltjin@chem.ecnu.edu.cn (L. Jin).

0304-3894/$ – see front matter © 2006 Elsevier B.V. All rights reserved.
doi:10.1016/j.jhazmat.2006.06.003

the efficient photocatalytic degradation. One way was to try to enhance the crystallinity integrality of TiO_2 particles. The accepted opinion was that in this case the recombination center of photogenerated carriers was minished and the separation effect of them was improved [22]. Another one was to explore the new composite semiconductor oxides as photocatalysts. They made the photogenerated carriers transport among the different energy levels of different semiconductor oxides and then separate well to prolong the carriers' life, which eventually enhanced the quantum efficiency [23,24].

In this study, a TiO_2/Ti mesh electrode was prepared in a composite process, which was the anodization procedure combined with laser-assisted annealing. The resulting TiO_2 film was investigated by XRD, AFM and EIS. MB was employed as reference for photooxidation investigation under UV irradiation. The objective of the study was to determine the photodegradation efficiency of the proposed TiO_2/Ti mesh electrode under different experimental conditions and also to compare the electrode with those prepared by different methods during PEC oxidation.

2. Experimental

2.1. Reagents

Titanium (purity > 99.7%, in area 3 cm × 3 cm) was purchased from the Far East Ti Equipment Co., Shanghai, China. MB and other chemicals were obtained from Shanghai Chemical Reagent Co., China. All reagents were used with analytical reagent grade. All solutions were prepared with doubly distilled water.

2.2. Device

A Verdi 5 laser (Coherent Co.; wavelength of 532 nm, output power from 0.01 to 5500 mW) was used to achieve the deposition of TiO_2 film. The X-ray diffraction measurements were performed in a D8ADVANCE X-ray diffractometer (Bruker axs Co., Germany) with a Cu Kα radiation source. Atomic force micrograph (AFM) was obtained by an AJ-I (Shanghai AJ Nanoscience Development Co. Ltd.).

The EIS measurements were carried out by a CHI660 electrochemical workstation system (CHI Co., USA). The conventional three-electrode electrochemical system was used in PEC oxidation experiment and EIS measurements, which was composed of a saturated calomel electrode (SCE) as the reference electrode, a platinum wire as the auxiliary electrode and one of the variously treated TiO_2/Ti mesh electrodes as the working electrode.

The PEC oxidation experiment was accomplished in a photoreactor system (as shown in Fig. 1), which was composed of a 15 mL quartz cell, a potentiostat (Jiangsu Electroanalytical Co., China) and a 36 W mercury UV lamp with a maximum irradiation peak at 254 nm.

2.3. Preparation of TiO_2/Ti mesh electrode

Titanium mesh was cleaned with HF acid and then rinsed with distilled water before it was anodized in a solution of 0.5 M H_2SO_4. The anodization process was carried out in two stages using the Ti mesh as the anode and a platinum plate as the cathode, respectively. In the first stage, an electrical current with the density of 100 mA cm^{-2} was applied to the anodization until the anode-to-cathode voltage was raised to 150 V. Subsequently, a 150 V voltage was given to the two poles unchangeably while the current density decreased to 40 mA cm^{-2} [19]. The freshly prepared TiO_2 mesh electrode was rinsed with distilled water and then dried at room temperature. Finally, the mesh electrode was swept by a 2.0 mm diameter laser beam at the rate of 2.0 mm s^{-1} for 30 min.

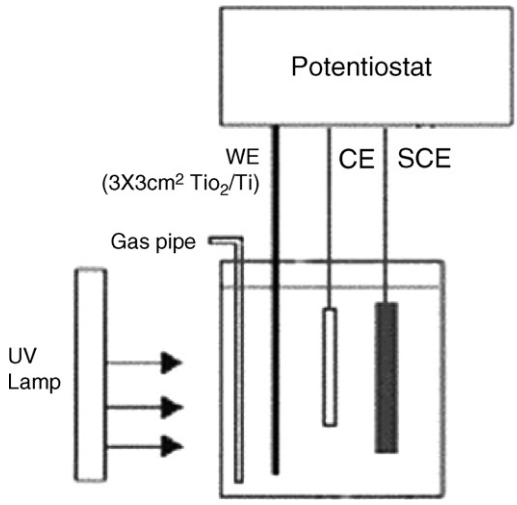

Fig. 1. Schematic diagram of photoelectrocatalytic reactor.

2.4. Photooxidation of MB

0.02 g/L MB and 0.1 M Na_2SO_4 (electrolyte) were added into the quartz reactor and the original pH of the solution was adjusted to 10.0 by the addition of NaOH or H_2SO_4. The TiO_2/Ti mesh electrode, a SCE and a Pt wire were placed in the reactor and connected with the potentiostat as typical three-electrode system. The photoelectrocatalytic degradation of MB was performed with a potentiostat and UV light. Air was pumped to the reactor through a gas pipe, which could help to mix the solution.

2.5. Analytical methods

The UV absorbance of MB was recorded by a Cary 50 Probe UV/visible spectrophotometer (Varian, USA) at 664 nm. The COD concentration was measured by COD standard method.

3. Results and discussion

3.1. Degradation of MB during PEC oxidation

When the TiO_2 photoelectrode was illuminated with UV light, a great number of electrons would be excited from valence band (VB) into conduction band (CB) by absorbing UV light quanta, leaving highly oxidative holes in VB and forming negative sites in CB, as shown in Fig. 2B(1). Meanwhile,

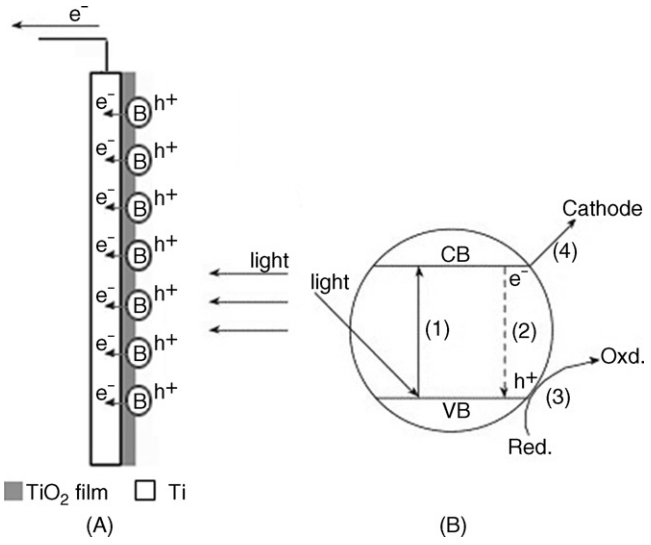

Fig. 2. Schematic representation of photocurrent generation from the macroscopic (A) and microscopic (B) views.

the photogenerated holes and electrons could recombine as observed in Fig. 2 B(2), which restrained the charge transfer and led to the efficiency debase of the photocatalytic oxidation. In the photochemical cell, the efficiency of this process was improved by applying a suitable anodic potential to the circuit owing to the conducting titanium substrate. The photogenerated holes reacted with adsorbed water (or OH^-) to produce hydroxyl radicals which could oxidize the organic compounds at the anode surface (Fig. 2B(3)), while the photogenerated electrons were transferred to the acceptor at the metallic cathode through the external electrical circuit (Fig. 2B(4)). The whole reaction process viewed on both macroscopic and microscopic scales was shown in Fig. 2.

MB was oxidized by applying an electrical bias of +0.5 V to the electrodes under UV irradiation for 150 min. The MB solutions were taken out to collect their UV absorbance data once every 30 min. Fig. 3 illustrated UV–vis absorbance changes of MB on TiO_2/Ti mesh electrode against irradiation time. Besides the UV absorbance, the COD removal could be another

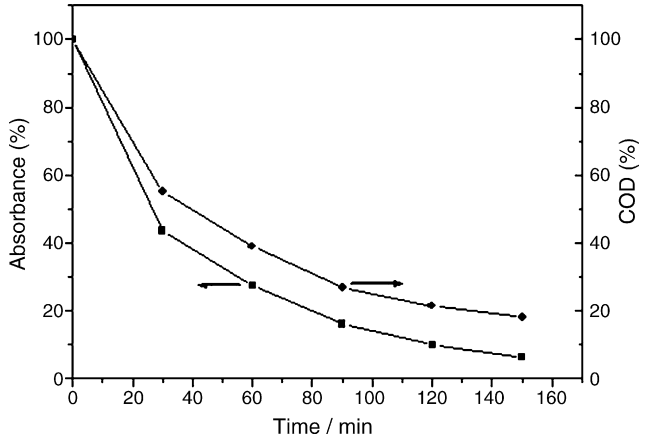

Fig. 3. Degradation of MB during PEC oxidation, in which MB initial concentration of 0.02 g/L and electrical bias +0.5 V (vs. SCE).

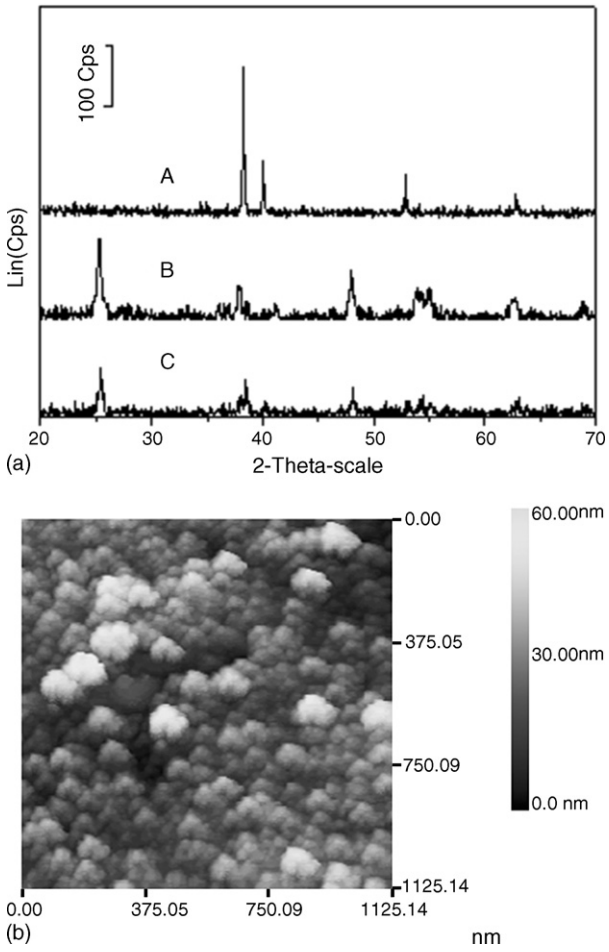

Fig. 4. The characteristics of TiO_2 film: (A) XRD patterns of Ti substrate (a), TiO_2 film calcined by laser (b) and by oven (c), respectively. (B) AFM image of TiO_2 film calcined by laser.

index of degradation extent. Therefore, the deduction of UV_{664} absorbance and COD recorded following irradiation time were presented in Fig. 3. During the first 30 min, the amount of the degraded MB was the most. Thereafter, the degradation reaction gradually decelerated. The results demonstrated that the degradation of MB after 150 min PEC oxidation was significantly fulfilled in the aspect of the reduction of UV absorbance and COD concentration.

3.2. *The characteristics of TiO_2 film*

The XRD patterns of raw titanium mesh, the TiO_2 films deposited on the titanium substrate by different heating methods were shown in Fig. 4(A). The oriented diffraction peaks were observed at $2\theta = 25.2°$, 37.8° and 48.0°. This revealed that the TiO_2 film consisted of anatase phase primarily. Additionally, the peak intensity of the film calcined by laser was greater than that by oven (dried at 105 °C for half an hour after anodization [19]), which implied that the crystallinity integrality of the laser-treated TiO_2 film was higher than the latter one.

The prepared TiO_2 film by laser calcination was observed with AFM. As presented in Fig. 4(B), it was seen clearly that the diameter of the particles was about 50 nm.

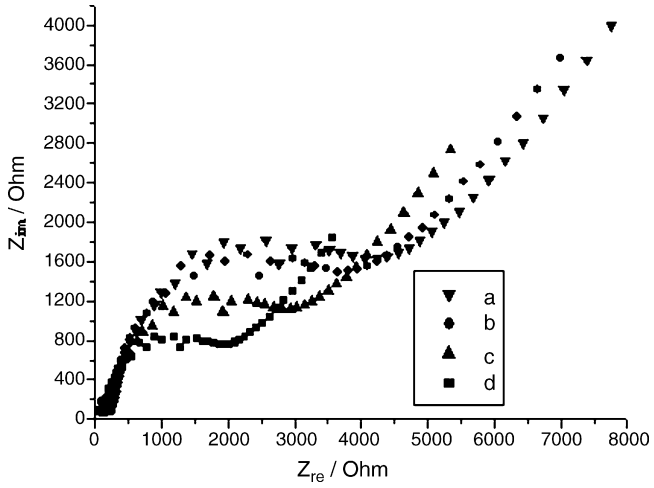

Fig. 5. Nyquist diagrams (Z_{im} vs. Z_{re}) for different TiO_2/Ti photoelectrodes. (a) The electrode prepared by laser, in the dark; (b) the electrode prepared by furnace, in the dark; (c) the electrode prepared by furnace, under UV illumination; (d) the electrode prepared by laser, under UV illumination. Detecting electrolyte: 0.1 M KCl, 0.1 M $K_3[Fe(CN)_6]/K_4[Fe(CN)_6]$ (1:1). ACI parameters: potential bias 0.15 V (vs. SCE), frequency range from 10^5 Hz to 1.0 Hz.

3.3. Electrochemical impedance spectroscopy analysis

The electrochemical impedance spectroscopy (EIS) was a powerful tool for studying the PEC activity on TiO_2 electrodes [25]. EIS measurement was carried out covering the 1 Hz–100 kHz frequency interval using a potential of 0.15 V. According to conventional double-layer theories, the impedance of the metal covered with an undamaged coating was very high and purely capacitive, which represented a straight vertical line intersecting the horizontal axis in the complex plane plot (Z_{im} versus Z_{re}). However, the electrical double-layer at the solid electrode behaved as a frequency distribution impedance instead of a pure capacitance due to the surface heterogeneity. The Nyquist plot for a typical Randles cell, which arose from the charge transfer reaction, was always a semicircle; Warburg impedance, where semi-infinite diffusion was the rate-determining step, appeared as a linear line with a slope of 45°.

Fig. 5 represented the Nyquist plots for the different electrodes obtained in the dark and under illumination in the presence of 0.1 M ferri/ferrocyanide redox couple in a 0.1 M KCl solution. All the diagrams were similar, including a semicircle part and a straight-line part. The semicircle at high frequencies was characteristic of the charge transfer process and the linear part at low frequencies corresponded to the diffusion-controlled step. In the dark, the plots for the two TiO_2 electrodes were very similar and their charge transfer resistance R_{ct}, equal to the diameter of the semicircle, were both assumed to be about 4000 Ω. However, once applied the UV light irradiation on them, R_{ct} of laser-treated TiO_2 electrode system (ca. 2000 Ω) was much less than R_{ct} of oven-treated TiO_2 electrode system (ca. 3000 Ω). The difference between the two electrodes under irradiation was great which attributed to the crystallinity of the TiO_2 film. The laser energy was so high that the crystallinity integrality of the formed TiO_2 film was enhanced when compared with the oven-treated TiO_2 film. Consequently, the recombination center of photogenerated carriers was minished and the separation effect of them was improved. So the laser-treated TiO_2 electrode system exhibited the higher activity of photocatalytic oxidation.

3.4. Selection of applied potential

There were two factors which affected the produced photocurrent: (i) anodic potential which was the force for photoelectrons to transport across TiO_2 film; (ii) photoelectrons as current carrier. When anodic potential was low, the effect of anodic potential on photoelectrons was dominating, so photoelectrons initially increased with the increment of potential bias. As anodic potential increased, a large amount of current carrier (photoelectrons) passed through the TiO_2 film. When the transportation and creation of photoelectrons reached equilibrium, photocurrent was saturated. Additionally, photogenerated holes were consumed by organic compounds in the solution, which facilitated the creation of photoelectrons. Therefore, with the increment of MB concentration, photocurrent was increscent, and the equilibrium potential was positive shift.

In order to select appropriate potential, linear sweep voltammetry was performed under different operating conditions. Fig. 6 showed the voltammograms of MB with different concentration using UV illumination. When the experiment was carried out without illumination (in the dark), the anodic current was small and was not affected by applied potential. Under irradiation, the anodic photocurrent increased initially with potential bias then reached saturation. The corresponding saturated potential increased with the increment of MB concentration. However, when the anodic potential went beyond +0.50 V, the photocurrent under each condition seemed to approach a limiting value for higher potentials gradually. Thus, a potential bias of +0.50 V was selected for all the PEC experiments.

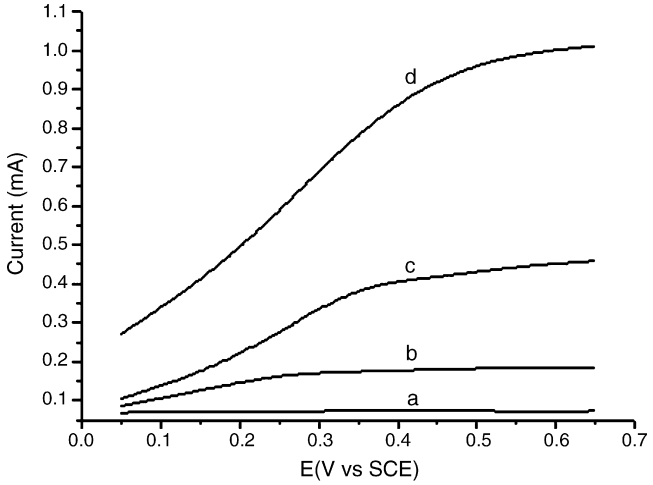

Fig. 6. The typical voltammograms of MB at TiO_2/Ti photoelectrode with and without UV illumination in 0.1 M Na_2SO_4 containing different concentrations of MB at pH 10.0: (a) without MB in dark; (b) without MB under illumination; (c) 0.01 g/L MB under illumination; (d) 0.025 g/L MB under illumination.

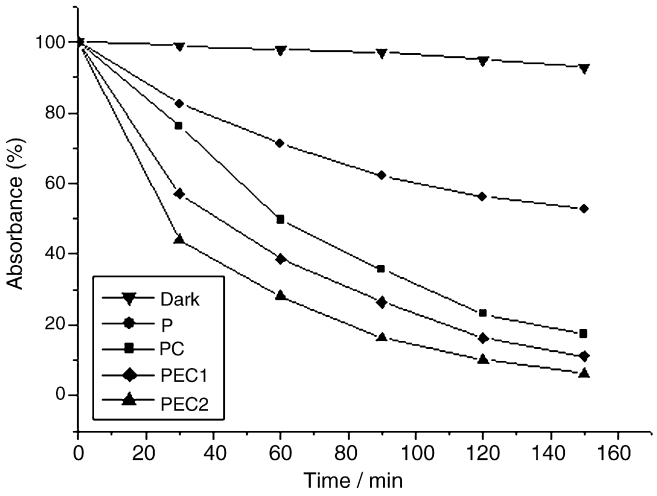

Fig. 7. The reduction of UV absorbance percentage at 664 nm with MB initial concentration of 0.02 g/L at pH 10.0 under different conditions.

3.5. Photooxidation of MB under different experimental conditions

To study the key factors affecting the photodegradation of MB, a series of tests were executed under different experimental conditions in which the deduction of UV absorbance was estimated. The experimental results were shown in Fig. 7. Test 1 (dark) was carried out in a dark condition with the TiO_2/Ti mesh electrode. Despite of a slight decrease of UV absorption at the early stage of Test 1 due to adsorption of MB by the TiO_2/Ti mesh electrode, almost 90% of MB remained in solution. Test 2 (P) was conducted under UV irradiation without the electrodes. It was seen that the UV absorbance reduced conspicuously so that Test 3 (PC) was performed under UV irradiation using the TiO_2/Ti mesh electrode but without any potential bias. The significant reduction of UV absorbance was observed. After 150 min degradation, about 80% of MB was removed. Test 4 (PEC1) was carried out under UV irradiation using the TiO_2/Ti mesh electrode prepared by oven with a potential voltage of 0.5 V. It was obvious that the reduction rate of UV was faster than Test 3. Test 5 (PEC2) was similar to Test 4 except for the electrode, which was prepared by laser as mentioned above. It was found that the UV absorbance decreased more than that in Test 4.

The investigation on the kinetics of MB degradation in aqueous solution under UV light irradiation was performed and UV absorbance deduction rate was assumed to follow an apparent first-order model as the following equation:

$$\ln(A_0/A_t) = kKt = k_{app}t \quad (1)$$

The UV absorbance had an exponential relationship to reaction time and the apparent first-order rate constant k_{app} could be calculated from Eq. (1). Table 1 listed k_{app} and the correlation coefficient R of the linear regression equation at different experimental conditions. The experimental results indicated that the reaction rate of MB degradation in the PEC oxidation using the laser-treated TiO_2/Ti mesh electrode was the fastest among all the reactions.

Table 1
Photooxidation of MB under different experimental conditions

	k_{app} (min^{-1})	Correlation coefficient, R	D_t (%)	D_e (%)	S (%)[a]
PEC1	0.0144	0.9982	88.8	68.0	76.6
PEC2	0.0178	0.9949	97.3	82.0	87.5
PEC-$_{P25}$	0.0156	0.9965	92.2	75.6	82.0
PC	0.0120	0.9981	82.5	59.1	71.6
PC-$_{P25}$	0.0108	0.9890	73.6	49.9	67.8
P	0.0043	0.9858	47.3	30.9	65.3
Dark	0.0005	0.9783	7.2	1.6	22.2

[a] $S = D_e/D_t \times 100\%$.

The UV absorbance could be used to illustrate the degradation of MB. However, MB could not undergo complete degradation to produce CO_2 and H_2O, as a result the intermediates were produced during the process. In order to show the degradation of organisms including MB and its intermediates produced more effectively, COD removal was also investigated. As shown in Fig. 8, the deduction of COD concentration varied in different tests. The specific trend of decrease was similar to but less obvious than that of UV absorbance. Initially, the degradation rates of all tests were outstanding except Test 1 (dark). The COD removal occurred slowly in all tests after 2 h irradiation.

From the analysis above, it was demonstrated that Test 5 (PEC2) was the most efficient to mineralize MB from the point view of UV absorbance or COD removal. Through the comparison between Test 4 and Test 5, it could be found that the TiO_2/Ti mesh electrode used in Test 5, prepared by the laser-assisted anodization method, had a higher photocatalytic activity than that electrode created by classical oven calcination.

3.6. Capability of complete mineralization

The products of the photodegradation of MB were complicated, including many kinds of intermediates and compounds,

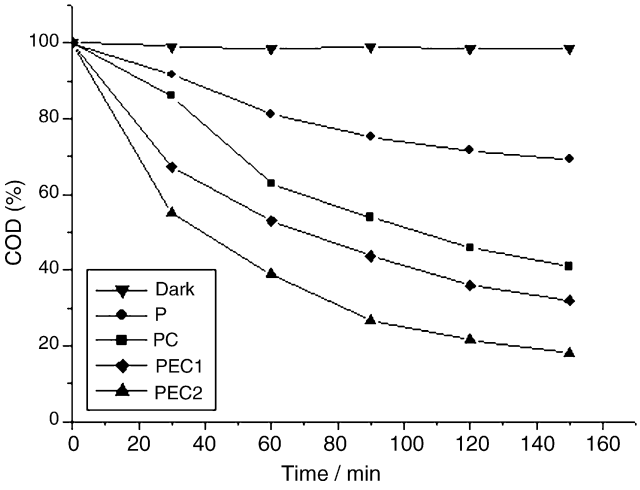

Fig. 8. The changes of COD concentration percentage with MB initial concentration of 0.02 g/L at pH 10.0 under different conditions.

which may not exhibit UV absorption property at 664 nm. Generally, it was anticipated that MB could be degraded to small inorganic matters such as carbon dioxide and water, which were friendly to our environment. Thus, COD removal was employed to express the effective degradation after UV illumination for 150 min ($D_e = [COD]_t/[COD]_0$). On the other hand, D_t, as total degradation percentage of MB, was calculated from UV absorbance changes ($D_t = A_t/A_0$, $t = 150$ min). The capability of complete mineralization of the tests performed above was denoted by S, which was the ratio of D_e to D_t as shown in the following equation:

$$S = D_e/D_t \times 100\% \quad (2)$$

Table 1 showed the values of D_t, D_e and S of different tests. Test 5 (PEC2) showed the greatest capability of deep oxidation of MB, which also exhibited the highest values of D_t and D_e. It was concluded that the TiO_2/Ti mesh electrode prepared by laser calcination had superiority to the typically oven-treated TiO_2/Ti mesh electrode and photoelectrocatalytic degradation was an effective method to completely mineralize the organic dye.

Test 6 (PEC-$_{P25}$) and Test 7 (PC-$_{P25}$) were conducted by the Ti mesh electrode fabricated with P25-TiO_2 nanoparticles [26], which were under the same experimental conditions with Test 5 and Test 3, respectively. From the results shown in Table 1, it was deduced that the photocatalytic activity of the TiO_2/Ti mesh electrode prepared by laser-treated was better than Ti mesh electrode treated by P25-TiO_2 nanoparticles.

4. Conclusions

In this paper, a TiO_2/Ti electrode was obtained by anodic oxidation combined with laser heating and examined by XRD, AFM and EIS, and it illuminated that the proposed electrode mainly consisted of anatase TiO_2 nanoparticles on its surface and exhibited superior photocatalytic. A series of experiments under different conditions were carried out to study the photocatalytic behavior of the laser-treated electrode. The comparing experiment results demonstrated that the photoelectrocatalysis using the proposed TiO_2 electrode could degrade MB most efficiently in terms of UV absorbance at 664 nm and COD removal after an irradiation time of 150 min. The application of electrical bias between the anode and cathode enhanced the PEC oxidation efficiency and +0.5 V was optimal. This TiO_2 electrode, which was also helpful for the efficiency improvement of PEC oxidation, was superior to the electrodes by different methods in the terms of the first-order kinetic constant and the capability of complete mineralization.

Acknowledgements

This work is supported by the National Natural Science Foundation of the People's Republic of China (No. 20327001), the Key Technology Research and Development Program of China (No. 2004BA210A07) and PhD Program Scholarship Fund of ECNU 2006.

References

[1] H. Zollinger (Ed.), Color Chemistry: Synthesis, Properties and Applications of Organic Dyes and Pigments, 2nd revised ed., VCH, 1991.
[2] A. Houas, H. Lachheb, M. Ksibi, E. Elaloui, C. Guillard, J.M. Hermann, Photocatalytic degradation pathway of methylene blue in water, Appl. Catal. B: Environ. 31 (2001) 145–157.
[3] A. Bianco-Prevot, C. Baiocchi, M.C. Brussino, E. Pramauro, P. Savarino, V. Augugliaro, G. Marci, L. Palmisano, Photocatalytic degradation of Acid Blue 80 in aqueous solutions containing TiO_2 suspensions, Environ. Sci. Technol. 35 (2001) 971–976.
[4] C. Galindo, P. Jacques, A. Kalt, Photochemical and photocatalytic degradation of an indigoid dye: a case study of Acid Blue 74 (AB74), J. Photochem. Photobiol. A: Chem. 141 (2001) 47–56.
[5] P. Cooper, Removing colour from dyehouse wastewaters—a critical review of technology available, J. Soc. Dyers Colour 109 (1993) 97–100.
[6] I.K. Konstantinou, T.A. Albanis, TiO_2-assisted photocatalytic degradation of azo dyes in aqueous solution: kinetic and mechanistic investigations. A review, Appl. Catal. B: Environ. 49 (2004) 1–14.
[7] N.H. Ince, D.T. Gonenc, Treatability of a textile azo dye by UV/H_2O_2, Environ. Technol. 18 (1997) 179–185.
[8] F. Zhang, J. Zhao, T. Shen, H. Hidaka, E. Pelizzetti, N. Serpone, TiO_2-assisted photodegradation of dye pollutants. II. Adsorption and degradation kinetics of eosin in TiO_2 dispersions under visible light irradiation, Appl. Catal. B: Environ. 15 (1998) 147–156.
[9] S. Irmak, E. Kusvuran, O. Erbatur, Degradation of 4-chloro-2-methylphenol in aqueous solution by UV irradiation in the presence of titanium dioxide, Appl. Catal. B: Environ. 54 (2004) 85–91.
[10] W.H. Leng, Z. Zhang, J.Q. Zhang, Photoelectrocatalytic degradation of aniline over rutile TiO_2 Ti electrode thermally formed at 600 °C, J. Mol. Catal. A: Chem. 206 (2003) 239–252.
[11] P.A. Carneiro, M.E. Osugi, J.J. Sene, M.A. Anderson, M.V.B. Zanoni, Evaluation of color removal and degradation of a reactive textile azo dye on nanoporous TiO_2 thin-film electrodes, Electrochim. Acta 49 (2004) 3807–3820.
[12] J. Zhao, T. Wu, K. Wu, K. Oikawa, H. Hidaka, N. Serpone, Photoassisted degradation of dye pollutants. 3. Degradation of the cationic dye Rhodamine B in aqueous anionic surfactant/TiO_2 dispersions under visible light irradiation: evidence for the need of substrate adsorption on TiO_2 particles, Environ. Sci. Technol. 32 (1998) 2394–2400.
[13] A. Fernandez, G. Lassaletta, V.M. Jimenez, A. Justo, A.R. Gonzalez-Elipe, J.M. Herrmann, H. Tahiri, Y. Ait-Ichou, Preparation and characterization of TiO_2 photocatalysts supported on various rigid supports (glass, quartz and stainless steel). Comparative studies of photocatalytic activity in water purification, Appl. Catal. B: Environ. 7 (1995) 49–63.
[14] G. Liu, T. Wu, J. Zhao, H. Hidaka, N. Serpone, Photoassisted degradation of dye pollutants. 8. Irreversible degradation of Alizarin Red under visible light radiation in air-equilibrated aqueous TiO_2 dispersions, Environ. Sci. Technol. 33 (1999) 2081–2087.
[15] P.A. Christensen, T.P. Curtis, T.A. Egerton, S.A.M. Kosa, J.R. Tinlin, Photoelectrocatalytic and photocatalytic disinfection of *E. coli* suspensions by titanium dioxide, Appl. Catal. B: Environ. 41 (2003) 371–386.
[16] X.Z. Li, F.B. Li, C.M. Fan, Y.P. Sun, Photoelectrocatalytic degradation of humic acid in aqueous solution using a Ti/TiO_2 mesh photoelectrode, Water Res. 36 (2002) 2215–2224.
[17] D. Jiang, H. Zhao, S. Zhang, R. John, Kinetic study of photocatalytic oxidation of adsorbed carboxylic acids at TiO_2 porous films by photoelectrolysis, J. Catal. 223 (2004) 212–220.
[18] J. Chen, M. Liu, L. Zhang, J. Zhang, L. Jin, Application of nano-TiO_2 towards polluted water treatment combined with electro-photochemical method, Water Res. 37 (2003) 3815–3820.
[19] X.Z. Li, H.L. Liu, P.T. Yue, Photoelectrocatalytic oxidation of Rose Bengal in aqueous solution using a Ti/TiO_2 mesh electrode, Environ. Sci. Technol. 34 (2000) 4401–4406.
[20] F.Y. Oliva, L.B. Avalle, E. Santos, O.R. Cámara, Photoelectrochemical characterization of nanocrystalline TiO_2 films on titanium substrates, J. Photochem. Photobiol. A: Chem. 146 (2002) 175–188.

[21] G. Colon, M.C. Hidalgo, J.A. Navio, Photocatalytic behaviour of sulphated TiO_2 for phenol degradation, Appl. Catal. B: Environ. 45 (2003) 39–50.

[22] R. Palombaria, M. Ranchellaa, C. Rola, G.V. Sebastiani, Oxidative photoelectrochemical technology with Ti/TiO_2 anodes, Sol. Energy Mater. Sol. Cells 71 (2002) 359–368.

[23] R. Vogel, P. Hoyer, H. Weller, Quantum-sized PbS, CdS, Ag_2S, Sb_2S_3, and Bi_2S_3 particles as sensitizers for various nanoporous wide-bandgap semiconductors, J. Phys. Chem. 98 (1994) 3183–3188.

[24] K.R. Gopidas, M. Bohorquez, P.V. Kamat, Photophysical and photochemical aspects of coupled semiconductors: charge-transfer processes in colloidal cadmium sulfide–titania and cadmium sulfide–silver(I) iodide systems, J. Phys. Chem. 94 (1990) 6435–6440.

[25] W.H. Leng, Z. Zhang, J.Q. Zhang, C.N. Cao, Investigation of the kinetics of a TiO_2 photoelectrocatalytic reaction involving charge transfer and recombination through surface states by electrochemical impedance spectroscopy, J. Phys. Chem. B 109 (2005) 15008–15023.

[26] M. Liu, S.A. Cheng, M. Wu, H.J. Zhang, W.Z. Li, C.N. Cao, Photoelectrocatalytic degradation of sulfosalicylic acid and its electrochemical impedance spectroscopy investigation, J. Phys. Chem. A 104 (2000) 7016–7020.